Indian Journal of Pure & Applied Physics
Vol. 55, May 2017, pp. 345-348

Optical fiber cone taper tip sensor for refractive index measurement

Vanita Bhardwaj & Vinod Kumar Singh*

Department of Applied Physics, Indian Institute of Technology (Indian School of Mines), Dhanbad, Jharkhand 826 004, India

Received 7 September 2015; revised 25 February 2017; accepted 14 March 2017

Optical fiber cone taper (OFCT) tip for refractive index sensing based on Michelson interferometer (MI) has been reported in present work. The fiber tip has been fabricated using chemical etching techniques, where hydrofluoric acid (HF) has been used as chemical etchant and silicone oil as protective layer for single mode fiber. The variation between intensity and refractive indices have been studied for small volume of liquid at operating wavelength 1550 nm and 1310 nm. In addition OFCT tips have been tested for pH detection and time response. The refractive index sensitivity of 9878.28 dB RIU^{-1} has been observed for sodium chloride (NaCl) solution in water of refractive index range from 1.3330 to 1.3342. Such kind of sensors using optical fiber tips are of low cost, simple fabrication and compact structure with high sensitivity.

Keywords: Optical fiber cone tapered tips, Chemical etching, Refractive index, pH sensing

1 Introduction

Refractive index sensors, based on tapered optical fiber configurations, have attracted many researchers over the last few decades. These configurations can be fabricated using various techniques such as fusion splicer[1,2], core-diameter mismatch[3,4], flame heating[5], fibers pulling[6], chemical etching methods[7-9], etc. Many researchers have reported various optical fiber sensing applications on the basis of tapered configurations[10-12]. The fiber configurations with different core/cladding diameters create the taper region. Recently we have reported some tapered configurations for temperature and refractive index sensing using down taper[13,14], core diameter mismatch[15] and core-offset structure[16]. For Mach-Zehnder interferometer (MZI) fabrication another types of fiber taper configuration was also used by Wang *et al.*[17] in which photonic crystal fiber (PCF) was spliced between two sections of single mode fiber (SMF) with air holes at splice points as reported. These configurations have various advantages over conventional sensors because of easy fabrication, high sensitivity with fast response, good stability, reproducibility and small size. These advantages of tapered configuration make them excellent candidate in physical, chemical and biological sensing. In addition, optical fiber tips based sensors has been found many applications in medicines and other biological field with compact structure over other optical fibers with different optical components.

Highly sensitive refractive index (*RI*) sensor of small volume liquid based on Michelson interferometer has been proposed and demonstrated in this study. The sensing head is fabricated by splicing a short section of SMF with OFCT tip. The cone angle of fiber tips is dominant factor that defines the quality of the fiber tip geometry. The sensitivity of the sensor probe is dependent on optical fiber tip. The OFCT tip is fabricated by using chemical etching technique which does not require any sophisticated nano-structure mentioned in previous work[18,19]. In chemical etching process HF is used as etchant and silicone oil as protective layer for SMF. These fiber probes show higher sensitivity to external *RI* of liquid than normal optical fiber sensors.

2 Sensor Head Fabrication using OFCT Tip

The SMF with core/cladding diameter 8.5/125 μm, silicone oil and HF were used for OFCT tip fabrications. Prior to chemical etching technique the plastic buffer jacket of optical fiber was stripped away using razor and then properly cleaned with ethanol. After that the SMF fiber was immersed normally into two phase liquid of volume 1.5 mL of HF having 40 % concentration and 0.5 mL of silicone oil. Because of lower density silicone oil forms upper layer where as HF remains in the bottom of the container. Here in this technique, the silicone oil is used to

*Corresponding author (E-mail: singh.vk.ap@ismdhanbad.ac.in)

prevent vaporization of acid and due to this, meniscus force helps to produce an OFCT tip. The capillary force helps to lift the acid-oil layer so that it raises in the fiber region, hence more surface of the fiber is exposed in contact of HF. Since the capillary force is inversely proportional to the fiber radius, as the acid etches the fiber resulting radius of fiber decreases. This decreased radius brings down the acid- oil layer slowly below the fiber tip and stops further etching of fiber as shown in Fig. 1.

After 70 min of etching process, the cone shaped fiber tip was obtained. Then the fabricated fiber tip was washed by water and ethanol to remove the acid residue. To make this fiber tip formation repeatable, the external environment like temperature, concentration and composition of the etchant and silicone oil remains same. The scanning electron microscopic image of fabricated tip is shown in Fig. 2.

3 Operating Principle

When light propagates to the tapered tip end of optical fiber it divides into two beams and after that one beam (B_1) propagates back shown in Fig. 3 and this reflected beam acts as sensing arm of MI. The other light beam (B_2) is reflected back which acts as reference arm of MI. The phase difference between two light beams caused due to the changes in external refractive index of core and cladding can be expressed by:

$$\Phi = \frac{4\pi \Delta n_{eff}}{\lambda} L \quad \ldots (1)$$

where Δn_{eff} represents the effective refractive index between core and cladding, λ is wavelength of light and L is the length of interferometer[20,21].

Generally, SMF supports lower order modes but the tapering of SMF helps to support higher order modes because of the refractive index difference between core and the surrounding medium. This results the high fraction of power in the evanescent field. The evanescent light can be easily scattered by surrounding medium, which affects the transmitted light and can be easily monitored by the detector. The reduction of core diameter increases the evanescent field and enhances the interaction of transmitted light with surrounding medium. Here V number of taper fiber becomes less than unity, because of the small core diameter due to tapered fiber. Thus the guided light is detected by cladding. Here original cladding of SMF acts as core and the surrounding medium acts

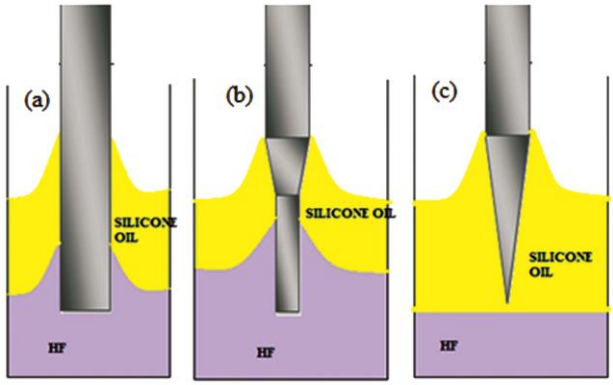

Fig. 1 – Schematic of cone tapered fiber probe fabrication at different time of itching (a) 30 min, (b) 45 min and (c) 70 min

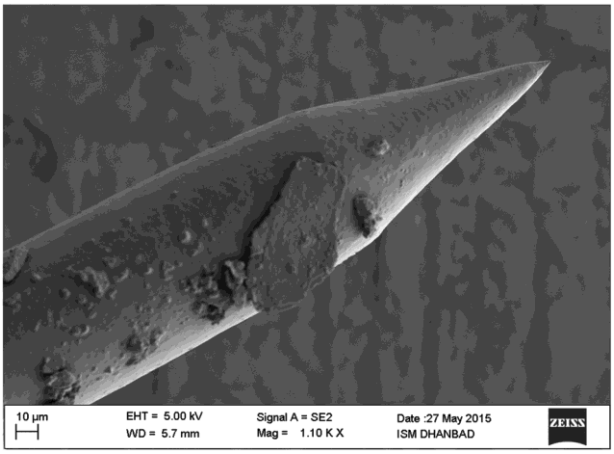

Fig. 2 – Scanning electron microscopic image of optical fiber cone taper tip

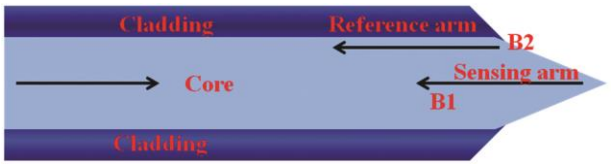

Fig. 3 – Schematic structure diagram of OFCT tip sensor

as cladding of the tapered fiber. V number for tapered fiber can be defined as[22,23]:

$$V_{\text{clad}}(z) = \frac{2\pi b(z)}{\lambda} \sqrt{{n_{clad}}^2 - {n_{surrounding\ medium}}^2} \quad \ldots (2)$$

where n_{clad} is the refractive index of cladding and $n_{surrounding\ medium}$ is refractive index of surrounding medium, $b(z)$ is the tapered region of fiber.

4 Results and Discussion

To investigate various sensing applications using OFCT tip, an experimental set up is schematically shown in Fig. 4. The laser with operating wavelength

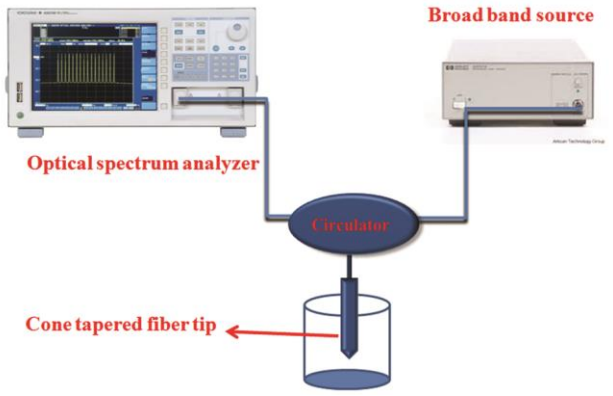

Fig. 4 – Schematics of the experimental setup for OFCT tip sensor

1550 nm and 1310 nm was used as light source and optical spectrum analyzer (OSA) was used to monitor the output optical power. A circulator was used to connect sensor with light source and OSA. When light propagating through lead in SMF reaches the splice joint, it splits into two parts one travelled through core and other from cladding region. The propagating modes are reflected back when they reaches at the OFCT tip end. The changes in surrounding *RI* cause the changes in output intensity. For the intensity measurement the OFCT tip was immersed into the solution of different concentrations. To ensure the repeatability of the present sensor, the experiment was repeated three times at room temperature.

The external *RI* of environment is changed from 1.3330 to 1.3342 by controlling the concentration ratio of NaCl and the *RI* of the core of fiber used in present work is 1.47. The incident light coming from light source is focused at the tip region for low *RI* because of high index contrast between core and the environment. With increasing *RI* of external environment, the index difference becomes small to confine light in fiber tip. The output intensity for operating wavelength 1550 nm and 1310 nm are shown in Figs 5 and 6. It can be seen from the plot that the change in intensity with *RI* is almost linear. The sensitivities of 8947.082 dB RIU^{-1} and 9878.28 dB RIU^{-1} are obtained at operating wavelength 1310 nm and 1550 nm, respectively. The obtained result is higher than the previously published work[24,25]. The behavior of result obtained for both operating wavelength are same and the output decreases with increment of *RI*. The tapering of SMF redefined the core/cladding of SMF in such a way that the tapered SMF acts as multimode fiber. This results the interaction of evanescent field so that the small

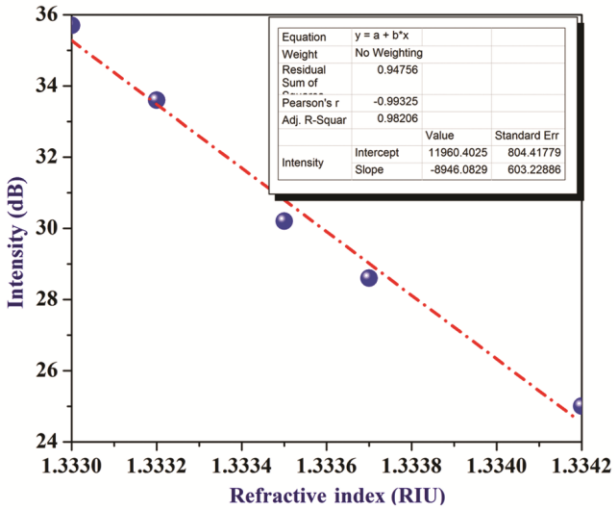

Fig. 5 – Change in intensity with function of refractive index

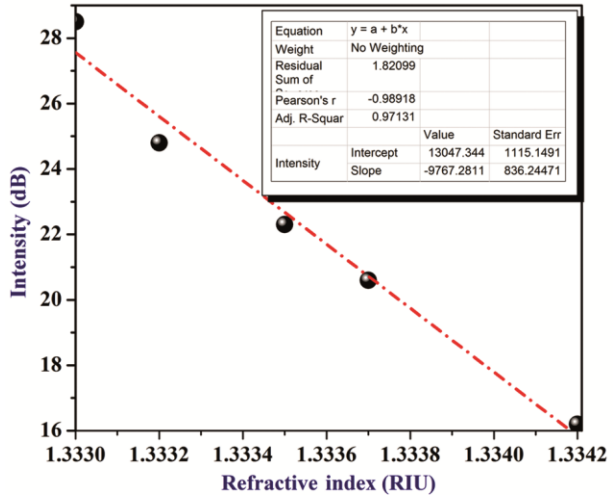

Fig. 6 – Change in intensity with refractive index

changes in the surrounding medium affects the transmitted optical power. The increase in NaCl concentration in water causes the decrease in intensity due to absorption of evanescent field[26].

The result is fitted with a linear trend where the value of R^2 is 0.9820 which confirms the best fitting for the obtained result. The change of liquid *RI* with time and pH sensing of liquid are also investigated by using same sensor probe. Evaporation rate measurement of methanol and water solution is shown in Fig. 7. The methanol used has a refractive index of 1.3395 at 10% concentration. Since the evaporation of methanol is much higher than water, the *RI* of methanol and water concentration decreases with time. Thus intensity of light also increases with time and the result comes stable with water.

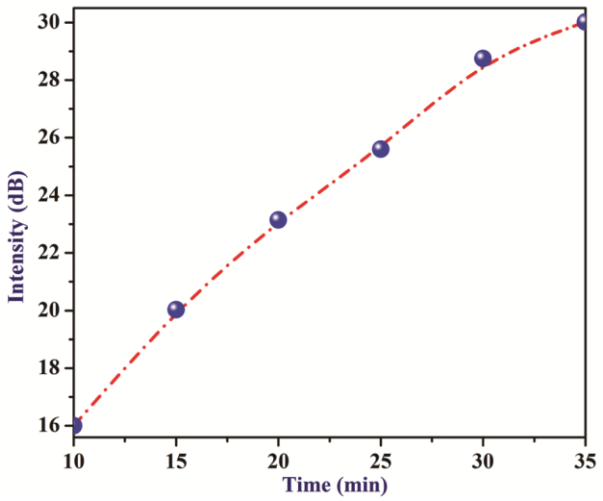

Fig. 7 – Intensity as a function of time for methanol/water mixtures 10% concentration

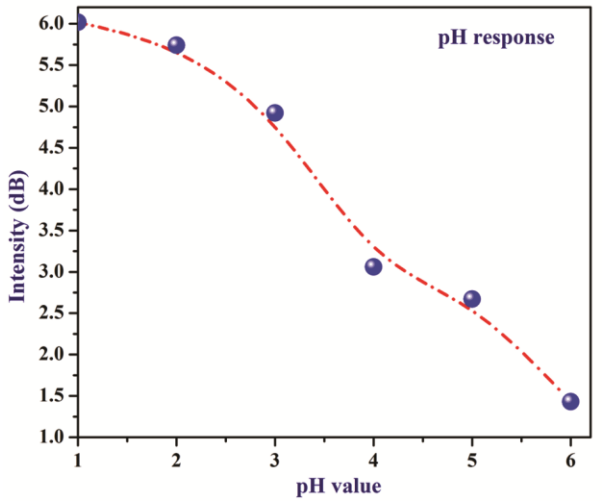

Fig. 8 – Relation between intensity with different pH value of acetic acid

Figure 8 shows the application of this sensor for pH sensing. The refractive index of acetic acid used for pH sensing is 1.3788. The low pH value is also tested for this sensor. The pH-value of acetic acid as a function of intensity is shown in Fig. 8. Figure 8 illustrates the variation of intensity with pH value of acetic acid at different concentrations. Variation of intensity with pH value proves that with increasing pH value of acetic acid the output intensity decreases. The sensitivity of 0.972 dB pH^{-1} was observed. These kinds of sensor for pH sensing are simple and have faster response than conventional pH meter.

5 Conclusions

A compact and low cost cone shape fiber tip sensor was proposed and demonstrated for refractive index sensing. The refractive index sensitivity values obtained for operating wavelength 1310 nm and 1550 nm were 8947.082 dB RIU^{-1} and 9878.28 dB RIU^{-1}, respectively, with linear behavior. The pH sensing effect of the fabricated fiber probes was also investigated and the sensitivity of 0.972 dB pH^{-1} was observed. As fabricated fiber probe is metal free, it can be used for many solutions. The proposed sensing structure has the advantages of the measurement of refractive index in small volume of liquid.

Acknowledgment

Authors are very thankful to Indian Institute of Technology (Indian School of Mines), India for providing financial support and research facilities to carry out this research work.

References

1 Dong S, Pu S & Wang H, *Opt Express*, 22 (2014) 19108.
2 Pu S & Dong S, *IEEE Photon J*, 6 (2014) 5300206.
3 Monzone Hernandez D, David M M, Villatoro J & Goncal B, *Sens Actuators B*, 125 (2007) 66.
4 Zhang C, Ning T, Li J, Pei L, Li C & Lin H, *Opt Fiber Technol*, 33 (2017) 71.
5 Verma R K, Sharma A K & Gupta B D, *Opt Commun*, 281 (2008) 1486.
6 Bariain C, Ignacio R M, Francisco J A & Manuel L A, *Opt Eng*, 39 (2000) 2241.
7 Banerjee A, *Sens Actuators B*, 123 (2007) 594.
8 Mukherjee A, *Sens Actuators B*, 145 (2010) 265.
9 Chenari Z, Latifi H, Ghamari S, Hashemi R S & Doroodmand F, *Opt Laser Technol*, 76 (2016) 91.
10 Raji Y M, Lin H S, Ibrahim S A, Mokhtar M R & Yusoff Z, *Opt Laser Technol*, 86 (2016) 8.
11 Lin H Y, Huang C H, Cheng G L, Chen N K & Chui H C, *Opt Express*, 20 (2012) 21693.
12 Deng M, Liu D & Li D, *Sens Actuators A*, 211 (2014) 55.
13 Bhardwaj V & Singh V K, *Sens Actuators A*, 244 (2016) 30.
14 Bhardwaj V, Gangwar R & Singh V K, *Opt Eng*, 55 (2016) 126107.
15 Bhardwaj V, Kishor K & Singh V K, *Plasmonics*, (2016) DOI 10.1007/s11468-016-0473-1.
16 Bhardwaj V & Singh V K, *Sens Actuators A*, 254 (2017) 95.
17 Wang J N & Tang J L, *Sensors*, 12 (2012) 2983.
18 Milenko K, *Opt Lett*, 37 (2012) 8.
19 Teng C, Yu F, Jing N & Zheng J, *Opt Fiber Technol*, 31 (2016) 32.
20 Yuan L, Yang J & Sun J, *Opt Lett*, 31 (2006) 2692.
21 Zhou J, Wang Y, Liao C, Yin G, He J & Sun B, *Asia Communications and Photonics Conference, (*2014) AF3F.5.
22 Leung A, Rijal K, Mohana P S & Mutharasan R, *Biosens Bioelectron*, 21 (2006) 2202.
23 Zhu S, Pang F & Wang T, *SPIE-OSA-IEEEI*, 8311 (2011) 83112B-1.
24 Tan Y C, Ji W B, Mamidala V, Chow K K & Tjin S C, *Sens Actuators B*, 270 (2014) 197.
25 Zhou J, *Sens Actuators B*, 208 (2015) 315.
26 Tian Y, Wang W, Wu N, Zou X & Wang X, *Sensors*, 11 (2011) 3780.